AGU PUBLICATIONS

Geophysical Research Letters

RESEARCH LETTER
10.1002/2017GL075020

Key Points:
- Magnetospheric expansion precedes erosion in response to a southward IMF turning
- Directional discontinuity crosses the magnetosheath in ~14 min
- Directional discontinuity significantly decelerates near the magnetopause

Supporting Information:
- Supporting Information S1

Correspondence to:
A. A. Samsonov,
a.samsonov@spbu.ru

Citation:
Samsonov, A. A., Sibeck, D. G., Dmitrieva, N. P., & Semenov, V. S. (2017). What happens before a southward IMF turning reaches the magnetopause? *Geophysical Research Letters*, *44*, 9159–9166. https://doi.org/10.1002/2017GL075020

Received 20 JUL 2017
Accepted 26 AUG 2017
Accepted article online 1 SEP 2017
Published online 22 SEP 2017

What Happens Before a Southward IMF Turning Reaches the Magnetopause?

A. A. Samsonov[1], D. G. Sibeck[2], N. P. Dmitrieva[1], and V. S. Semenov[1]

[1]Earth's Physics Department, St. Petersburg State University, St. Petersburg, Russia, [2]Code 674, NASA Goddard Space Flight Center, Greenbelt, MD, USA

Abstract Previous observations have shown a ~10–15 min time delay in the ionospheric response to solar wind directional discontinuities marked by either southward or northward interplanetary magnetic field (IMF) turnings. We have studied one southward IMF turning observed by Time History of Events and Macroscale Interactions during Substorms (THEMIS) and GOES in the dayside magnetosphere. Using a global MHD model, we have reproduced the magnetopause motion in this event. We find that the observed delay in the ground response can be completely explained by deceleration of the directional discontinuity in the subsolar magnetosheath. We show that the speed of the discontinuity significantly decreases in the vicinity of the magnetopause where the magnetic barrier formed during the previous northward IMF interval. The southward turning can reach the magnetopause only after complete disruption of the magnetic barrier. The disruption or dissipation occurs via magnetosheath reconnection, as confirmed by high-speed jets in the magnetosheath. The magnetopause moves sunward as the directional discontinuity transits the magnetosheath. This sunward motion is followed by the earthward motion when the discontinuity strikes the magnetopause and magnetopause reconnection begins.

1. Introduction

The orientation of the interplanetary magnetic field (IMF) is one of the crucial parameters that control the dynamics of the magnetospheric-ionospheric (MI) system. Although we know in general the behavior of the magnetosphere for steady northward and steady southward IMF orientations, the transient processes that occur when the IMF rotates from northward(southward) to southward(northward) orientation are still not well understood. One of the unresolved issues concerns the transition time between the two states. Continuous multipoint ground observations from ground magnetometers and radars may better characterize transition processes in the magnetosphere than scattered spacecraft observations; therefore, the transition times have mostly been estimated using ground data. Previous estimations often took the starting point as the time when directional discontinuities, abbreviated as DD, (whether tangential or rotational discontinuities, but sometimes also interplanetary shocks) encountered the magnetopause, and the final point as the first response seen in ionospheric convection and/or ground magnetic field variations. Since solar wind data were usually taken far upstream of the bow shock, various methods were applied to estimate the time lag between the solar wind monitor (often near the Lagrangian point L1) and the subsolar magnetopause. While the speed and orientation of DDs in the pristine solar wind are reasonably assumed to be constant, the propagation speed through the magnetosheath varies and it may results in discrepancies as we will show below.

Spreiter et al. (1966) gasdynamic model predicts velocities in the dayside magnetosheath to vary from about 0.3 V_{SW} downstream of the bow shock to zero at the subsolar magnetopause. Using Spreiter et al.'s model, Freeman and Southwood (1988) estimated the time lag between solar wind and magnetosheath observations and compared it with observations. They pointed out that the time lag increases when the magnetosheath spacecraft moves from the outer magnetosheath toward the magnetopause.

Nishida (1968) was first to estimate the transition time using ground magnetic field data and obtained, on average, a 7 min time lag between the crossing of an DD through the nose of the bow shock and the associated magnetic variations on the ground. Clauer and Banks (1986) and Knipp et al. (1991) obtained an estimate for the transition time (but measured from the time of contact with the subsolar magnetopause) of 15 min. Etemadi et al. (1988) and Todd et al. (1988) studied the dependence of the ionospheric response time on magnetic local time and found the most rapid responses of about 4-5 min in the noon and midafternoon

sectors. Saunders et al. (1992) studied the changes in dayside ionospheric convection that occur in response to long-period IMF B_z oscillations and found an average first response in the noon sector of 7–10 min after the estimated time at the subsolar magnetopause. Hairston and Heelis (1995) concluded that the time lag varies from 17 to 25 min for five cases with northward-to-southward turnings, but it was 28 and 44 min for two opposite (southward-to-northward) turnings.

Taylor et al. (1998) used high-resolution Super Dual Auroral Radar Network (SuperDARN) observations during a southward-to-northward turning case to obtain a prompt response in the form of a patch of sunward flow near noon within ~2 min. It should be noted, however, that Taylor et al. (1998) estimated the propagation time of the tangential discontinuity (bringing this B_z variation) from the bow shock to the magnetopause as 8 min, so they assumed a significant deceleration of the discontinuity in the magnetosheath. Also, using SuperDARN data, Ruohoniemi and Greenwald (1998) derived the transition time from the magnetopause to the first ionospheric response as about 14 min, but this response almost immediately (in ~2 min) expands to cover all observed sectors of magnetic local time. Using ionospheric convection changes derived from the assimilative mapping of ionospheric electrodynamics technique for 65 events, Ridley et al. (1998) obtained a communication time of 8 min. They also took into account deceleration in the magnetosheath but quantified it as 4 min. The superposed epoch analysis of Turner et al. (1998) showed that the high-latitude polar cap electric field observed by the Polar spacecraft began to change, on average, 10 min after discontinuities with southward turning reached the magnetopause. Using radar data, Huang et al. (2000) obtained delays of the first ionospheric response between 5 and 9 min, while the propagation time through the magnetosheath was estimated as 8 min. In a recent paper, Bhaskar and Vichare (2013) concluded that the communication time for signals associated with southward and northward IMF turnings to propagate from the subsolar bow shock to the ionosphere is 12 ± 6 min, while the ionospheric reconfiguration time is 10 ± 8 min.

Although the dispersion of the transition time estimates is large, summarizing more recent observational works, we conclude the following. If we add up the propagation time through the dayside magnetosheath and the time between the first contact of discontinuity with the magnetopause and the first visible ionospheric response, then the sum lies somewhere between 10 and 16 min. We should also note the large scatter of magnetosheath propagation time estimates in previous papers.

The interaction of DDs with the Earth's magnetosphere was simulated using the Integrated Space Weather Prediction Model in the series of papers (Maynard et al. 2001, 2002, 2007). These global MHD simulations agree well with observational results. In particular, Maynard et al. (2001) estimated the transition time, with the very first ionospheric response appearing 8 min after contact with the subsolar magnetopause, while clear large-scale changes in the ionospheric currents occur 4 min later. Explaining the time delay, the authors (following to Shepherd et al. (1999)) concluded that it requires a significant draping of the magnetic field lines in the magnetosheath before a magnetopause reconnection and corresponding ionospheric response occur.

Maynard et al. (2002) provided new details of the transition process and predicted magnetic reconnection in the magnetosheath. When the DD enters the magnetosheath, the decrease in the solar wind speed causes the discontinuity front to narrow and the electric current density on the front to increase. This initiates reconnection which was confirmed in the simulations by increases in speed in the exhaust direction, an *X* magnetic field configuration and dissipation electric fields at locations distant from the magnetopause (Maynard et al., 2002). When tangential discontinuities associated with significant increases (decreases) in the plasma density interact with the bow shock, then fast shocks (fast rarefaction waves) precede slightly modified tangential discontinuities in the magnetosheath (Maynard et al., 2007; Volk & Auer, 1974; Wu et al., 1993). Phan et al. (2007) in Cluster and Maynard et al. (2007) in Polar data confirmed the prediction for magnetosheath reconnection at DD current sheet. Retino et al. (2007) and Yordanova (2016) associated magnetosheath reconnection with turbulent structures, i.e., small-scale current sheets which may sporadically appear downstream from the quasi-parallel bow shock.

Although the aforementioned papers made significant progress toward understanding the magnetospheric response to DDs, we have reproduced one event with a global MHD model and found that some important details were missed in the picture described above. In particular, we will show below a magnetospheric expansion that precedes the magnetospheric compression and intensification of the magnetopause currents. This expansion may be observed in the magnetosphere and even on the ground. Moreover, we suggest another physical explanation for the transition time or the time delay in the ionospheric response which takes into account magnetosheath processes.

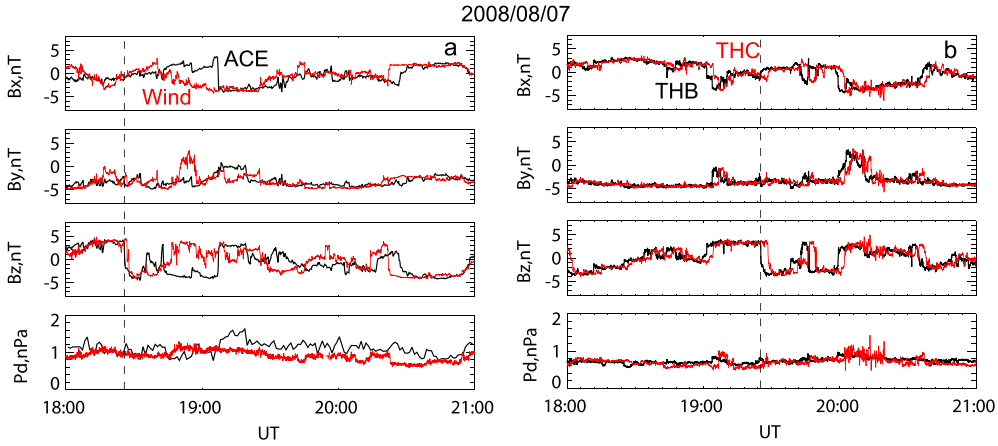

Figure 1. Interplanetary magnetic field and solar wind dynamic pressure from (a) ACE (black line) and Wind (red line) and (b) THEMIS B (black line) and THEMIS C (red line). Vertical dashed lines mark the selected discontinuity in ACE and THB data. The distance between ACE and THEMIS B along x axis is 203 R_E.

In this short letter, we present one event in which a DD characterized by a significant B_z change from positive to negative (a southward turning) impacts the magnetosphere. We have reproduced this event using the Space Weather Modeling Framework (SWMF) global MHD model (Tóth et al., 2005, 2012) available through Community Coordinated Modeling Center (CCMC) runs on request. We did not choose this event with the intention of finding unusual magnetopause behavior; instead, the only two selection criteria were a large and isolated B_z jump and good coverage by spacecraft with four solar wind monitors upstream of the bow shock and five spacecraft in the dayside magnetosphere.

2. A Puzzle in Event 7 August 2008

We examine solar wind plasma and IMF data from the Advanced Composition Explorer (ACE), Wind, The Time History of Events and Macroscale Interactions during Substorms (THEMIS) spacecraft, probes THEMIS B (THB), and THEMIS C (THC) for an event on 7 August 2008. The four spacecraft observed similar IMF and plasma variations during the selected time interval. We pay particular attention to a DD that passed ACE at 18:26 UT, Wind at 18:27 UT, THB at 19:25, and THC at 19:28 UT. Figure 1 shows the magnetic field components and solar wind dynamic pressure from the four spacecraft. We use GSM coordinates throughout the paper.

Both ACE and Wind were located near the L1 point with the distance separating them about 136 R_E, mainly in the GSM y direction. The large separation distance explains why some IMF variations have different shapes and are observed at different times by the two spacecraft; however, IMF variations around the selected discontinuity are very similar in both the ACE and Wind data. ACE was a little sunward from Wind and registered the discontinuity 1.5 min before. Through the discontinuity, IMF B_z varied sharply from about +4 to −4 nT, while the B_x and B_y remained nearly constant.

Both THB and THC were near the Earth but still upstream of the dayside bow shock. Figure S1 in the supporting information shows their positions and the positions of five magnetospheric spacecraft: THEMIS D (THD), THEMIS E (THE), Geostationary Operational Environmental Satellites (GOES) 10, GOES 11, and GOES 12. In particular, the THB GSM (X, Y, and Z) coordinates at 19:30 UT are (29, 2, and −6) R_E, the THC coordinates are (18, 3, and −5) R_E, THD coordinates are (10, 4, and −3) R_E, and GOES 11 coordinates are (6, −2, and −2) R_E. The distance between THB and THC was 11 R_E, and they observed very similar magnetic field structures with a time shift of 3 min.

We have determined the normal of the DD by applying the MVA method (Sonnerup & Cahill, 1967) to both THB and THC data and also using the timing method since we know the arrival times at the four spacecraft (Russell et al., 1983). Both methods give similar results, and the normal, with an accuracy of 15°, coincides with the GSE x axis. In particular, the timing method gives the normal (x, y, and z)=(0.98, −0.07, and 0.13) in GSM coordinates and a speed in the Earth's frame of 352 km/s. The latter is close to the average flow velocity seen at ACE, Wind, and THEMIS. Using THB data, we have found $Bn/B = 0.18$ and $\Delta(B)/B = 0.015$. Since both ratios

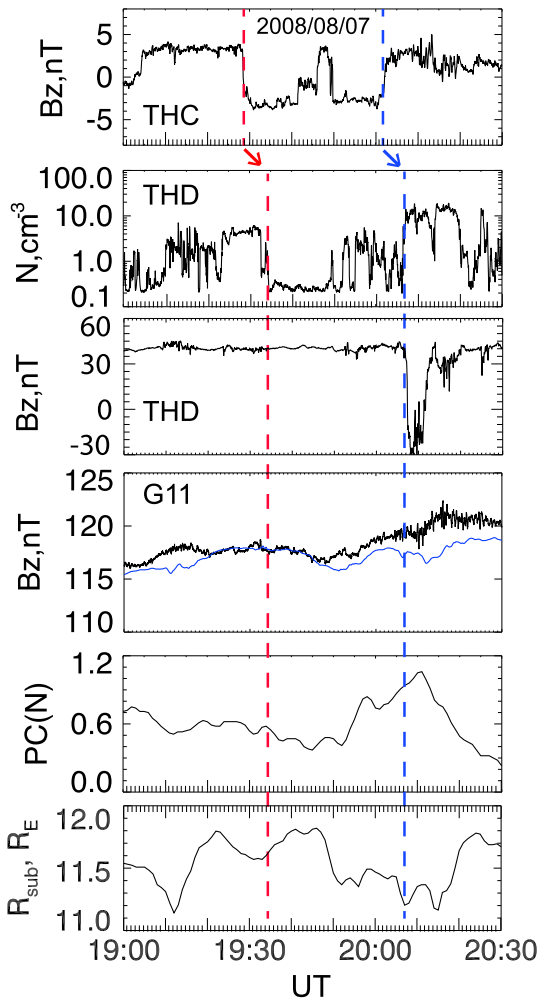

Figure 2. The IMF B_z from THEMIS C, the density and B_z from THEMIS D, the B_z from GOES 11 from observations (black) and MHD simulation (blue), the polar cap (north) index PCN, and the magnetopause radial distance along the Sun-Earth line obtained in the MHD simulations. Vertical red (blue) lines mark the southward (northward) IMF turning in the first panel and transition from LLBL to the magnetosphere proper (and return transition from the magnetosphere to the magnetosheath) observed by THD in the second panel.

are small, the discontinuity may be either a tangential or a rotational discontinuity. However, the variations of the magnetic field in the selected time interval correlate well with the variations of velocity (not shown) indicating Alfvén fluctuations, so we tend to think that it is a rotational discontinuity. The density changes insignificantly from the upstream to downstream state (with a small peak in the middle of the discontinuity) and is about 3.5 cm^{-3}.

THD and THE are situated near the subsolar magnetopause, with THD slightly farther from the Earth. Figure 2 shows IMF B_z from THC, density and B_z from THD, B_z from GOES 11, and the polar cap (north) index PCN (Troshichev et al., 2006). The last panel displays the magnetopause radial distance obtained in the MHD simulations. Red and blue vertical dashed lines in the top panel mark the solar wind DD with the southward turning discussed above and the next well-distinguished discontinuity with an opposite northward turning. Since THC is not far upstream of the bow shock ($x = 18\,R_E$), both solar wind discontinuities need only about 1 min to reach the nose of the bow shock and a few more minutes to cross the magnetosheath (at least, the most part of the magnetosheath as discussed below). Then, at ~19:34 UT, THD observed a decrease of the density and an increase of the temperature (only the density is shown) indicating magnetospheric expansion (see the shift in the red line in Figure 2). Probably, the spacecraft moved from the low-latitude boundary layer (LLBL) into the magnetosphere proper, because the magnetic field varied only slightly and remained close to typical magnetospheric values. The response to the northward IMF turning observed by THC at 20:02 UT is opposite, the density at THD increases at 20:07 UT, indicating the magnetospheric compression.

A magnetospheric expansion following a southward turning and a magnetospheric compression after a northward turning are opposite to what one expects on the basis of previous works. It has been well established (e.g., Aubry et al., 1970; Fairfield, 1971; Petrinec et al., 1991; Pudovkin et al., 1998; Sibeck et al., 1991) that the magnetopause lies closer to the Earth during southward IMF intervals than during northward intervals, on average. An initial interpretation of this magnetospheric erosion in terms of partial penetration of the southward magnetosheath magnetic field into the magnetosphere (Kovner & Feldstein, 1973) violates the frozen-in condition (Sibeck et al., 1991). A more physical explanation invokes intensification of either the Region 1 (Hill & Rassbach, 1975; Maltsev & Lyatsky, 1975) or nightside cross-tail currents (Wiltberger et al., 2003) in response to intervals of southward IMF orientation. Both current systems decrease dayside magnetic field strengths, allowing the dayside magnetopause to move earthward.

The behavior of B_z at GOES 11 and of the PCN index confirms, in general, our assumption about the expansion at 19:34 UT and the compression at 20:07 UT. B_z decreases until 19:48 UT but then increases after 19:49 UT. The PCN index is determined from ground measurements in the polar cap and usually correlates well with E_y the (responsible for reconnection) electric field at the dayside magnetopause. The PCN begins to increase only after 19:45 UT, but it decreases between 19:34 and 19:45 UT. This indicates a ~15 min delay in the ground response relative to the DD arrival time at the subsolar bow shock.

3. Can an MHD Model Help Solve This Puzzle?

We have simulated this event with the SWMF (BATS-R-US) global MHD model using solar wind input conditions from THB. Figure 2 compares IMF B_z at THEMIS C, density at THEMIS D, predicted and observed B_z variations at GOES 11, the ground-based PCN index, and the radial distance to the subsolar magnetopause predicted by the global MHD model. We used an internal CCMC routine to identify the magnetopause boundary between open and closed magnetic field lines. The model predicts an expanded magnetosphere between 19:33 and 19:41 UT and compressed magnetosphere between 19:46 and 19:52 UT in agreement with the weak and then enhanced B_z observed at GOES 11 and also with the density changes at THD. In particular,

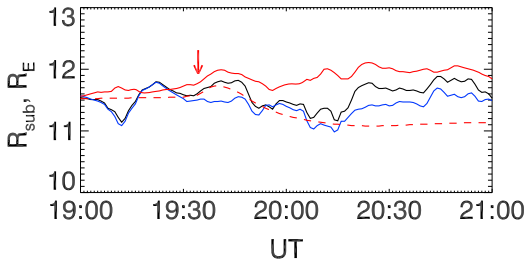

Figure 3. The radial distance to the magnetopause subsolar points in run 1 (black) with unchanged solar wind conditions from THB, in run 2 (blue), in which only the solar wind plasma parameters vary, in run 3 (red), in which only the IMF varies, and in run 4 (red dashed) with the only B_z change through the discontinuity. The red arrow indicates the time when the observed magnetospheric expansion begins.

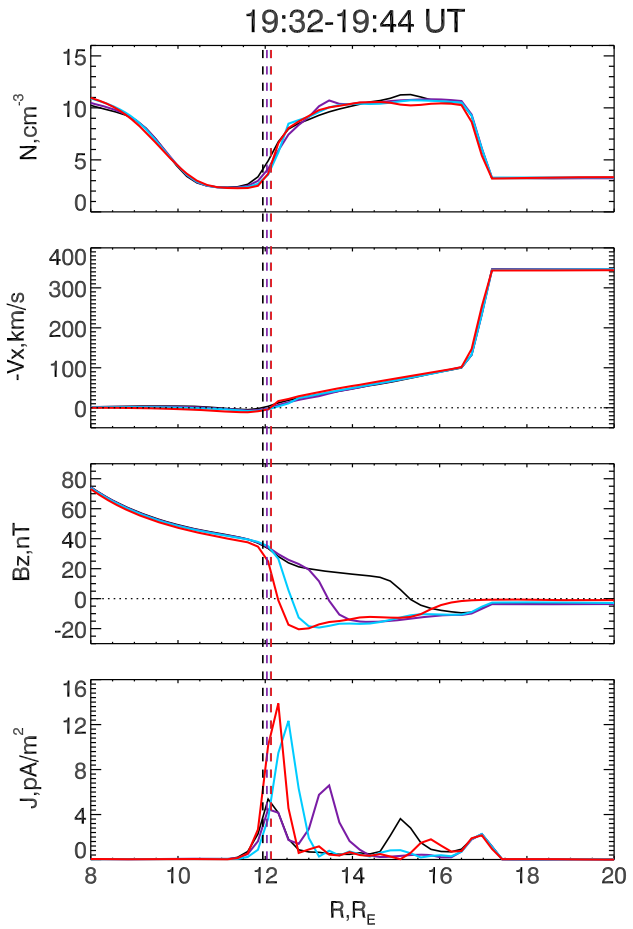

Figure 4. The density, velocity V_x, magnetic field B_z, and electric current density $|J|$ profiles along the Sun-Earth line at t = 19:32 UT (black), 19:36 UT (violet), 19:40 UT (blue), and 19:44 UT (red). Dashed vertical lines indicate the predicted magnetopause positions at the corresponding times as indicated in Figure 3, the subsolar distance monotonously increases from 19:32 to 19:44 UT, but the distances at 19:40 (blue) and 19:44 UT (red) almost coincide).

THD stayed in the magnetosphere proper between 19:34 and 19:49 UT, indicating a more expanded magnetosphere at that time. Thus, we conclude that the MHD model predicts the magnetospheric expansion nearly at the right time. The next question is how does the model explain this expansion?

The radial distance to the magnetopause depends on both the IMF B_z and solar wind dynamic pressure. Using MHD simulations, we can separate variations of R_{sub} caused by solar wind dynamic pressure changes and those related exclusively to IMF changes. We have made two simulation runs, in addition to run 1 with the solar wind conditions completely matching the THB data. For boundary conditions in run 2, we use plasma parameters (i.e., density, velocity, and temperature) observed by THB but keep the magnetic field constant. For boundary conditions in run 3, we use the observed IMF (actually varying only B_y and B_z but keeping B_x constant to avoid issues related to *div B* errors) and keep the plasma parameters constant. Moreover, we present results from run 4, in which the only change in input conditions during the whole time interval is the jump of B_z through the selected discontinuity. Figure 3 presents the subsolar distance R_{sub} for the four runs.

Over the whole interval, R_{sub} obtained from run 1 is better correlated with R_{sub} from run 2 than from run 3. However, the magnetospheric expansion at 19:33 UT indicated by the red arrow is predicted in runs 1 and 3 but missed in run 2. This means that the solar wind plasma parameters were nearly constant at this time (as indeed observed), and this particular expansion results solely from the IMF changes. Later, plasma parameter variations certainly influence R_{sub} in run 1. Using the results of runs 3 and 4, we can conclude that the magnetospheric expansion continues about 8 min and then the compression gradually begins. Results from run 4 illustrate the magnetopause behavior if both the solar wind plasma and IMF parameters are constant during the whole interval, with the only exception being B_z jump through the DD with the southward turning. The magnetopause erosion follows the initial expansion, and the final magnetopause position after a prolonged interval of southward IMF is closer to the Earth. In this particular case, R_{sub} decreases from 11.5 to 11.1 R_E (at 19:00 and 21:00 UT, correspondingly).

We have related the magnetospheric expansion to the IMF southward turning, but now we intend to understand the physical mechanism for the expansion. Figure 4 shows profiles for the density, V_x, B_z, and electric current density $|J|$ along the Sun-Earth line at 19:32 (black), 19:36 (violet), 19:40 (blue), and 19:44 (red) UT. We use the results of run 3 with a high spatial resolution of 1/8 R_E in the dayside magnetosheath and magnetosphere. At the initial time step, 19:32 UT, the DD lies at $x \simeq 15\,R_E$ in the outer magnetosheath. The outward magnetopause motion in the simulation begins a minute later. The electric current density has three clear maxima, the first is at the magnetopause ($\simeq$12 R_E), the second is at the DD, and the third is at the bow shock ($\simeq$17 R_E). Since the the initial magnetic field is northward, the magnetic field increases and the density decreases in the inner magnetosheath near the magnetopause. This particular region is called the magnetic barrier (Spreiter & Alksne 1969; Erkaev 1988) or the plasma depletion layer (Zwan & Wolf, 1976). Both names reflect properties of this region. However, the name magnetic barrier seems to be preferable, because it emphasizes the increase in the magnetic field which in turn results in diversion of plasma flow from the earthward direction to tangential along the magnetopause surface and it creates the plasma depletion.

At the next two times, the DD moves toward the magnetopause, and the magnetic barrier gradually dissipates. If we follow the point $B_z = 0$ at the

discontinuity front, it shifts from $x = 15.3$ at 19:32 UT through 13.4 (19:36 UT) and 12.6 R_E (19:40 UT) to 12.3 R_E (19:44 UT). Thus, the speed of the discontinuity decreases when approaching the magnetopause because the flow speed decreases and the northward magnetic barrier prevents the southward turning from rapid interacting with the magnetospheric field. The southward turning can reach the magnetopause only when the barrier is completely dissipated, and this process requires 8-10 min.

Indeed, the DD comes close to the magnetopause at 19:40 UT, but the maximum of the current density still lies about 0.4 R_E sunward of the predicted magnetopause position. Moreover, the electric current at the magnetopause ($R_{MP} = 12.1\ R_E$ as indicated by vertical blue line in Figure 4) at 19:40 UT is nearly the same as at 19:32 and 19:36 UT. The magnetopause current significantly increases only at the next time 19:44 UT, while the maximum of the electric current and the predicted magnetopause position (vertical red line) almost coincide. Therefore, we argue that the DD reaches the magnetopause only at 19:44 UT. The discontinuity crosses the magnetosheath about 14 min, from 19:30 to 19:44 UT.

We began the discussion of this event with a puzzle in the observations because the first response to the southward turning was an outward magnetopause motion opposite to our expectations of inward motion. According to the simulation, the dayside magnetopause began to move sunward when the DD crossed about half the width of the magnetosheath, i.e., nearly at the same time when the dissipation of the magnetic barrier begins. Samsonov et al. (2012) compared the total pressure at the subsolar magnetopause for northward and radial IMF conditions and found that the total pressure is higher in the northward case. They explained this numerical result by the existence of a magnetic barrier in the northward case. In the magnetic barrier the magnetic pressure rapidly increases, while the thermal pressure decreases; however, the total pressure, i.e., the sum of magnetic and thermal terms, gradually increases too. Figure S2 in the supporting information shows the variations of the magnetic and thermal pressures at the subsolar magnetopause. The dissipation of the magnetic barrier gradually decreases the total pressures at the magnetopause from 19:32 to 19:45 UT, mostly because of the decrease in the magnetic pressure.

The magnetic barrier dissipates via magnetic reconnection. The reconnection develops in the magnetosheath at the discontinuity front. This is confirmed by high-speed streams away from the Sun-Earth line along the z direction. The MHD simulation predicts these high-speed jets; however, space limitation forces us to postpone their description for the future.

4. Conclusions

We have studied and reproduced with MHD simulations one event on 7 August 2008. We have explored the magnetospheric response to a solar wind DD, which changes the IMF B_z from strongly positive to strongly negative. Since the IMF has been directed northward for at least 20 min before the discontinuity, a strong magnetic barrier is formed in the magnetosheath upstream of the dayside magnetopause. The simulation shows that the magnetic barrier significantly decelerates the earthward propagation of the discontinuity. While solar wind plasma usually crosses the magnetosheath in 2–3 min, the DD requires about 14 min to move from the bow shock to the magnetopause. It takes nearly 3 min to cross the outer magnetosheath but 11 min to move through the inner magnetosheath where the magnetic barrier is located. The DD deceleration in the magnetosheath completely explains the delay in the ionospheric response, because the ionospheric currents intensify at the time when the discontinuity actually reaches the magnetopause.

The simulation shows that the magnetopause moves outward as the magnetic barrier dissipates (while the DD transits the inner magnetosheath). The simulated magnetospheric expansion agrees with THD observations of the inner edge of the low-latitude boundary layer moving outward, the decrease of B_z seen by GOES 11 and the decrease of the PCN index in the ground data at ~19:34 UT. We explain this outward magnetopause motion as resulting from a decrease in the pressure applied to the magnetopause caused by the dissipation of the magnetic barrier. Note that the solar wind density changes insignificantly through the DD; therefore, the interaction of the DD with the bow shock results in neither a fast shock nor a fast compressional wave preceding the DD in the magnetosheath if the density changes (Volk & Auer, 1974). When the DD reaches the magnetopause, the outward magnetopause motion is followed by the inward motion expected due to magnetopause erosion.

The magnetic barrier near the magnetopause is dissipated via magnetosheath reconnection at the DD. The simulation shows high-speed jets transverse to the Sun-Earth line that moving earthward together with the

DD. We deliberately do not discuss the magnetosheath reconnection in this letter, but note that reconnection at narrowing DD current layers in the magnetosheath has been previously simulated and observed by Maynard et al. (2002, 2007) and Phan et al. (2007).

Although we have analyzed only one event, so far, we believe that our results are applicable for many similar events. We suppose that the two conditions in this case determine the magnetospheric behavior: (i) a 20 min interval of stable northward IMF precedes the DD during which the magnetic barrier has been formed and (ii) there is a significant IMF rotation through the discontinuity so the magnetic field direction in the magnetic barrier changes on more than 90°. It would be interesting to inspect DDs with other upstream and downstream IMF directions in order to understand the differences in magnetospheric response. We believe that the magnetic energy accumulated in the magnetic barrier during an interval with a stable IMF orientation should be converted by reconnection into the kinetic and thermal energy, if a solar wind directional discontinuity brings an opposite IMF orientation into the magnetosheath.

Acknowledgments
Simulation results have been provided by the Community Coordinated Modeling Center (http://ccmc.gsfc.nasa.gov) at Goddard Space Flight Center. ACE, Wind, and THEMIS data are available from the Coordinated Data Analysis Web (CDAWeb), from the THEMIS mission site (http://themis.ssl.berkeley.edu/), from ACE mission site (http://www.srl.caltech.edu/ACE/). A. A. S. work with THEMIS data at Goddard Space Flight Center was supported by THEMIS project. This work was supported by Russian Science Foundation Grant N14-17-00072.

References

Aubry, M. P., Russell, C. T., & Kivelson, M. G. (1970). Inward motion of the magnetopause before a substorm. *Journal of Geophysical Research*, *75*(34), 7018–7031. https://doi.org/10.1029/JA075i034p07018

Bhaskar, A., & Vichare, G. (2013). Characteristics of penetration electric fields to the equatorial ionosphere during southward and northward IMF turnings. *Journal of Geophysical Research: Space Physics*, *118*, 4696–4709. https://doi.org/10.1002/jgra.50436

Clauer, C. R., & Banks, P. M. (1986). Relationship of the interplanetary electric field to the high-latitude ionospheric electric field and currents Observations and model simulation. *Journal of Geophysical Research*, *91*, 6959–6971. https://doi.org/10.1029/JA091iA06p06959

Erkaev, N. V. (1988). Results of research on MHD flow past the magnetosphere (Review). *Geomagnetism and Aeronomy*, *28*, 529–541.

Etemadi, A., Cowley, S. W. H., Lockwood, M., Bromage, B. J. I., & Willis, D. M. (1988). The dependence of high-latitude dayside ionospheric flows on the north-south component of the IMF — A high time resolution correlation analysis using EISCAT "Polar" and AMPTE UKS and IRM data. *Planetary and Space Science*, *36*, 471–498. https://doi.org/10.1016/0032-0633(88)90107-9

Fairfield, D. H. (1971). Average and unusual locations of the Earth's magnetopause and bow shock. *Journal of Geophysical Research*, *76*(28), 6700–6716. https://doi.org/10.1029/JA076i028p06700

Freeman, M. P., & Southwood, D. J. (1988). The correlation of variations in the IMF with magnetosheath field variations. *Advances in Space Research*, *8*, 217–220. https://doi.org/10.1016/0273-1177(88)90134-2

Hairston, M. R., & Heelis, R. A. (1995). Response time of the polar ionospheric convection pattern to changes in the north-south direction of the IMF. *Geophysical Research Letters*, *22*, 631–634. https://doi.org/10.1029/94GL03385

Hill, T. W., & Rassbach, M. E. (1975). Interplanetary magnetic field direction and the configuration of the day side magnetosphere. *Journal of Geophysical Research*, *80*(1), 1–6. https://doi.org/10.1029/JA080i001p00001

Huang, C.-S., Murr, D., Sofko, G. J., Hughes, W. J., & Moretto, T. (2000). Ionospheric convection response to changes of interplanetary magnetic field B_z component during strong B_y component. *Journal of Geophysical Research*, *105*, 5231–5244. https://doi.org/10.1029/1999JA000099

Knipp, D. J., Richmond, A. D., Emery, B., Crooker, N. U., de La Beaujardiere, O., & Evans, D. (1991). Ionospheric convection response to changing IMF direction. *Geophysical Research Letters*, *18*, 721–724. https://doi.org/10.1029/90GL02592

Kovner, M. S., & Feldstein, Y. I. (1973). On solar wind interaction with the Earth's magnetosphere. *Planetary and Space Science*, *21*, 1191–1211. https://doi.org/10.1016/0032-0633(73)90206-7

Maltsev, Y. P., & Lyatsky, W. B. (1975). Field aligned currents and erosion of the dayside magnetosphere. *Planetary and Space Science*, *23*, 1257–1260. https://doi.org/10.1016/0032-0633(75)90149-X

Maynard, N. C. (2001). Response of ionospheric convection to changes in the interplanetary magnetic field: Lessons from a MHD simulation. *Journal of Geophysical Research*, *106*, 21,429—21,452. https://doi.org/10.1029/ 2000JA000454

Maynard, N. C., Sonnerup, B. U. Ö., Siscoe, G. L., Weimer, D. R., Siebert, K. D., Erickson, G. M., … Heinemann, M. A. (2002). Predictions of magnetosheath merging between IMF field lines of opposite polarity. *Journal of Geophysical Research*, *107*(A12), 1456. https://doi.org/10.1029/2002JA009289

Maynard, N. C., Burke, W. J., Ober, D. M., Farrugia, C. J., Kucharek, H., Lester, M., … Siebert, K. D. (2007). Interaction of the bow shock with a tangential discontinuity and solar wind density decrease: Observations of predicted fast mode waves and magnetosheath merging. *Journal of Geophysical Research*, *112*, A12219. https://doi.org/10.1029/2007JA012293

Nishida, A. (1968). Coherence of geomagnetic DP 2 fluctuations with interplanetary magnetic variations. *Journal of Geophysical Research*, *73*(17), 5549–5559. https://doi.org/10.1029/JA073i017p05549

Petrinec, S. P., Song, P., & Russell, C. T. (1991). Solar cycle variations in the size and shape of the magnetopause. *Journal of Geophysical Research*, *96*(A5), 7893–7896. https://doi.org/10.1029/90JA02566

Phan, T. D., Paschmann, G., Twitty, C., Mozer, F. S., Gosling, J. T., Eastwood, J. P., … Lucek, E. A. (2007). Evidence for magnetic reconnection initiated in the magnetosheath. *Geophysical Research Letters*, *34*, L14104. https://doi.org/10.1029/2007GL030343

Pudovkin, M. I., Besser, B. P., & Zaitseva, S. A. (1998). Magnetopause stand-off distance in dependence on the magnetosheath and solar wind parameters. *Annales Geophysicae*, *16*(4), 388–396. https://doi.org/10.1007/s00585-998-0388-z

Retino, A., Sundkvist, D., Vaivads, A., Mozer, F., Andre, M., & Owen, C. J. (2007). In situ evidence of magnetic reconnection in turbulent plasma. *Nature Physics*, *3*, 235–238. https://doi.org/10.1038/nphys574

Ridley, A. J., Lu, G., Clauer, C. R., & Papitashvili, V. O. (1998). A statistical study of the ionospheric convection response to changing interplanetary magnetic field conditions using the assimilative mapping of ionospheric electrodynamics technique. *Journal of Geophysical Research*, *103*, 4023–4040. https://doi.org/10.1029/97JA03328

Ruohoniemi, J. M., & Greenwald, R. A. (1998). The response of high-latitude convection to a sudden southward IMF turning. *Geophysical Research Letters*, *25*, 2913–2916. https://doi.org/10.1029/98GL02212

Russell, C. T., Mellott, M. M., Smith, E. J., & King, J. H. (1983). Multiple spacecraft observations of interplanetary shocks: Four spacecraft determination of shock normals. *Journal of Geophysical Research*, *88*(A6), 4739–4748. https://doi.org/10.1029/JA088iA06p04739

Samsonov, A. A., Němeček, Z., Šafránková, J., & Jelínek, K. (2012). Why does the subsolar magnetopause move sunward for radial interplanetary magnetic field?. *Journal of Geophysical Research*, *117*, A05221. https://doi.org/10.1029/2011JA017429

Saunders, M. A., Freeman, M. P., Southwood, D. J., Cowley, S. W., Lockwood, M., Samson, J. C., … Hughes, T. J. (1992). Dayside ionospheric convection changes in response to long-period interplanetary magnetic field oscillations—Determination of the ionospheric phase velocity. *Journal of Geophysical Research*, *97*, 19,373–19,380. https://doi.org/10.1029/92JA01383

Shepherd, S. G., Greenwald, R. A., & Ruohoniemi, J. M. (1999). A possible explanation for rapid, large-scale ionospheric responses to southward turnings of the IMF. *Geophysical Research Letters*, *26*, 3197–3200. https://doi.org/10.1029/1999GL010670

Sibeck, D. G., Lopez, R. E., & Roelof, E. C. (1991). Solar wind control of the magnetopause shape, location, and motion. *Journal of Geophysical Research*, *96*(A4), 5489–5495. https://doi.org/10.1029/90JA02464

Sonnerup, B. U. O., & Cahill Jr., L. J. (1967). Magnetopause structure and attitude from Explorer 12 observations. *Journal of Geophysical Research*, *72*, 171–183. https://doi.org/10.1029/JZ072i001p00171

Spreiter, J. R., & Alksne, A. Y. (1969). Plasma flow around the magnetosphere. *Reviews of Geophysics*, *7*(1–2), 11–50. https://doi.org/10.1029/RG007i001p00011

Spreiter, J. R., Summers, A. L., & Alksne, A. Y. (1966). Hydromagnetic flow around the magnetosphere. *Planetary and Space Science*, *14*, 223–250. https://doi.org/10.1016/0032-0633(66)90124-3

Taylor, J. R., Cowley, S. W. H., Yeoman, T. K., Lester, M., Jones, T. B., Greenwald, R. A., … Hairston, M. R. (1998). SuperDARN studies of the ionospheric convection response to a northward turning of the interplanetary magnetic field. *Annales Geophysicae*, *16*, 549–565. https://doi.org/10.1007/s00585-998-0549-0

Todd, H., Cowley, S. W. H., Lockwood, M., Willis, D. M., & Luehr, H. (1988). Response time of the high-latitude dayside ionosphere to sudden changes in the north-south component of the IMF. *Planetary and Space Science*, *36*, 1415–1428. https://doi.org/10.1016/0032-0633(88)90008-6

Toth, G., van der Holst, B., Sokolov, I. V., Zeeuw, D. L. D., Gombosi, T. I., Fang, F., … Opher, M. (2012). Adaptive numerical algorithms in space weather modeling. *Journal of Computational Physics*, *231*(3), 870–903. https://doi.org/10.1016/j.jcp.2011.02.006

Troshichev, O., Janzhura, A., & Stauning, P. (2006). Unified PCN and PCS indices: Method of calculation, physical sense, and dependence on the IMF azimuthal and northward components. *Journal of Geophysical Research*, *111*, A05208. https://doi.org/10.1029/2005JA011402

Tóth, G., Sokolov, I. V., Gombosi, T. I., Chesney, D. R., Clauer, C. R., De Zeeuw, D. L., … Kóta, J. (2005). Space weather modeling framework: A new tool for the space science community. *Journal of Geophysical Research*, *110*, A12226. https://doi.org/10.1029/2005JA011126

Turner, N. E., Baker, D. N., Pulkkinen, T. I., Singer, H. J., Mozer, F., & Lepping, R. P. (1998). High-altitude polar cap electric field responses to southward turnings of the interplanetary magnetic field. *Journal of Geophysical Research*, *103*, 26,533–26,546. https://doi.org/10.1029/98JA01743

Volk, H. J., & Auer, R.-D. (1974). Motions of the bow shock induced by interplanetary disturbances. *Journal of Geophysical Research*, *79*(1), 40–48. https://doi.org/10.1029/JA079i001p00040

Wiltberger, M., Lopez, R. E., & Lyon, J. G. (2003). Magnetopause erosion: A global view from MHD simulation. *Journal of Geophysical Research*, *108*(A6), 1235. https://doi.org/10.1029/2002JA009564

Wu, B.-H., Mandt, M. E., Lee, L. C., & Chao, J. K. (1993). Magnetospheric response to solar wind dynamic pressure variations: Interaction of interplanetary tangential discontinuities with the bow shock. *Journal of Geophysical Research*, *98*, 21,297–21,311. https://doi.org/10.1029/93JA01013

Yordanova, E. (2016). Electron scale structures and magnetic reconnection signatures in the turbulent magnetosheath. *Geophysical Research Letters*, *43*, 5969–5978. https://doi.org/10.1002/2016GL069191

Zwan, B. J., & Wolf, R. A. (1976). Depletion of solar wind plasma near a planetary boundary. *Journal of Geophysical Research*, *81*(10), 1636–1648. https://doi.org/10.1029/JA081i010p01636